Thermal properties of the mixed spin-1 and spin-3/2 Ising ferrimagnetic system with two different random single-ion anisotropies

Accepted Manuscript

Thermal properties of the mixed spin-1 and spin-3/2 Ising ferrimagnetic system with two different random single-ion anisotropies

J.R.V. Pereira, T.M. Tunes, A.S. de Arruda, M. Godoy

PII: S0378-4371(18)30171-7
DOI: https://doi.org/10.1016/j.physa.2018.02.085
Reference: PHYSA 19205

To appear in: *Physica A*

Received date : 25 September 2017
Revised date : 4 January 2018

Please cite this article as: J.R.V. Pereira, T.M. Tunes, A.S. de Arruda, M. Godoy, Thermal properties of the mixed spin-1 and spin-3/2 Ising ferrimagnetic system with two different random single-ion anisotropies, *Physica A* (2018), https://doi.org/10.1016/j.physa.2018.02.085

Highlights:

- The phase diagram for the mixed spin-1 and spin-3/2 Ising ferrimagnetic system with two different random single-ion anisotropies was obtained.
- To investigate the system Monte Carlo simulations were used.
- Only second-order phase transition lines for any values of p and q was found.
- A multicompensation behavior for some values of p and q was observed.

Thermal properties of the mixed spin-1 and spin-3/2 Ising ferrimagnetic system with two different random single-ion anisotropies

J. R. V. Pereira
Instituto Federal de Educação, Ciência e Tecnologia de Mato Grosso, 78890-000, Sorriso, MT, Brazil.

T. M. Tunes
Instituto de Engenharia, Universidade Federal de Mato Grosso, 78060-900, Várzea Grande, MT, Brazil.

A. S. de Arruda* and M. Godoy†
Instituto de Física, Universidade Federal de Mato Grosso, 78060-900, Cuiabá, MT, Brazil.
(Dated: January 4, 2018)

In this work, we have performed Monte Carlo simulations to study a mixed spin-1 and spin-3/2 Ising ferrimagnetic system on a square lattice with two different random single-ion anisotropies. This lattice is divided in two interpenetrating sublattices with spins $S^A = 1$ in the sublattice A and $S^B = 3/2$ in the sublattice B. The exchange interaction between the spins on the sublattices is antiferromagnetic ($J < 0$). We used two random single-ion anisotropies, D_i^A and D_j^B, on the sublattices A and B, respectively. We have determined the phase diagram of the model in the critical temperature T_c versus strength of the random single-ion anisotropy D plane and we shown that it exhibits only second-order phase transition lines. We also shown that this system displays compensation temperatures for some cases of the random single-ion distribution.

I. INTRODUCTION

One of the most important and also interesting models of statistical mechanics is the Ising model. The simplicity of its variables, which assume values ± 1 (two states) makes it possible to model various systems (biological, social, economic, magnetic, etc.). Its generalization has led to other models with more than two states and with other types of interactions besides exchange interaction (J_{ij})[1–3]. Limiting only to the case of magnetic models, today there are several models constituted with different variables de spins, which are the well-known models of mixed-spins [4–7]. These mixed-spins models are used to describe the thermodynamic behavior of several new materials, such as $[Fe(C_5Me_5)_2][TCNE]$ molecular-based magnetic materials [8–10], nanowires [11–14].

The mixed-spin Ising model has in recent years been widely employed to study the theoretical aspects of ferrimagnet systems, where the phase diagram presents compensation temperature, in addition to multicritical behavior are much appreciated. In this model the system is represented by two interpenetrating sublattices of spins with different magnitudes. Here, the compensation temperature is the temperature (below the critical temperature T_c) in which the magnetization of one sublattice cancels completely the effects of the magnetization of other sublattice, causing the total magnetization to change signal. Of course, these systems are interesting not only from an academic point of view (both theoretical and experimental), but there is a boost due to technological applications: thermomagnetic recording, ultra-high-density magnetic recording media, light-emitting diodes, lithium-ion batteries, electronic and computer technologies, all due to their outstanding magnetic, electronic and optical properties. In this context, the study of the mixed-spin Ising model of different magnitudes had a great attraction. Basically the focus was on the mixed-spin system distributed in two sublattices, one with spins $S = 1/2$ and the other with spins $S > 1/2$ and with an additional crystalline field (single-ion anisotropy) and magnetic field. Thus, the systems formed by two sublattices with different spin types have been a strong candidate to model some types of ferrimagnetic and molecular-based magnetic materials. There are many studies on mixed-spin Ising systems that have been performed in different topologies and methods: effective-field theory (EFT)[15–25], mean-field approximation (MFA) [26–29], renormalization-group technique (RG) [30], Monte Carlo simulation (MC) [31–43] and Green's function technique [44, 45], etc. On the other hand, the effects of random single-ion anisotropy has been even less investigated, but in Refs. [46, 47] these effects are studied indicating the appearance of new characteristics in the thermodynamic properties of the systems. Souza et al. [29] obtained the phase diagram of the mixed spin-1 and spin-3/2 Ising ferrimagnetic system on a square lattice with two different random single-ion anisotropies using mean-field theory based on the Bogoliubov inequality for the Gibbs free energy.

Žukovič and Bobák [48] used MC simulation to explain the phase diagram and the thermodynamic properties of the mixed spin-1 and spin-3/2 Ising system with uniform single-ion anisotropy on a square lattice. They did not find a re-entrant phenomenon and additional first-order phase transition within the ordered ferrimagnetic phase, as predicted by mean filed approximations, and also the existence of a tricritical point at which the tran-

* aarruda@fisica.ufmt.br
† mgodoy@fisica.ufmt.br

sition would change from second-order to first-order one. They found the multicompensation behavior, with two compensation points observed. The purpose of this work is to investigate the mixed spin-1 and spin-3/2 Ising ferrimagnetic system with two different random single-ion anisotropies using MC simulations. This model is similar to the one studied in reference [29]. In this work, our main motivation is to contribute to the knowledge of the thermodynamic properties of the mixed-spin Ising ferrimagnetic model with random anisotropies, going beyond the mean field theory, such as the reference [29].

The paper is organized as follows: in Section II, we describe the mixed spin-1 and spin-3/2 Ising ferrimagnetic system and we present some details concerning the simulation procedures. In Section III, we described the results obtained. Finally, in the last Section, we present our conclusions.

II. THE MODEL AND SIMULATIONS

The mixed spin-1 and spin-3/2 Ising ferrimagnetic system consists of two interpenetrating square sublattices A, with spin-1 (states $S^A = 0, \pm 1$), and B with spin-3/2 (states $S^B = \pm 1/2, \pm 3/2$). In each site of the sublattices there is a random single-ion anisotropies D_i^A and D_j^B acting on the spin-1 and spins-3/2, respectively. This system is described by the following Hamiltonian model,

$$\mathcal{H} = -J \sum_{\langle i,j \rangle} S_i^A S_j^B - \sum_{i \in A} D_i^A (S_i^A)^2 - \sum_{j \in B} D_j^B (S_j^B)^2, \quad (1)$$

where the first term represents the interaction between the nearest neighbors spins on sites i and j located on the sublattices A and B, respectively. J is the magnitude of the exchange interaction, and the sum is over all nearest neighboring pairs of spins. Here, we have considered the antiferromagnetic exchange interaction, $J < 0$. The second and third terms represent the random single-ion anisotropies at all the sites of the sublattices A and B, respectively. Therefore, the sums are performed over $N/2$ spins of each sublattice.

The random single-ion anisotropies satisfy the following probability distributions:

$$P(D_i^A) = p\delta(D_i) + (1-p)\delta(D_i - D_i^A), \quad (2)$$

and

$$P(D_j^B) = q\delta(D_j) + (1-q)\delta(D_j - D_j^B), \quad (3)$$

where the term $p\delta(D_i)$ ($q\delta(D_j)$) indicated that one fraction p (q) of the spins on the sublattice A (B) are free of the influence of random single-ion anisotropies, while the terms $(1-p)\delta(D_i - D_i^A)$ ($(1-q)\delta(D_j - D_j^B)$) indicated that one fraction $(1-p)$ ($(1-q)$) of the spins on the sublattice A (B) are under to influence of the random single-ion anisotropies. Thus, for instance, the case $p = q = 0$ was studied using MC simulations in the reference [48], where all spins are subject to action of an uniform single-ion anisotropies $D^A = D^B \equiv D$. We have considered also here the case simplest where the random single-ion anisotropies on the sublattices have the same strength, i.e., $D_i^A = D_j^B \equiv D$, for each value of p and q. This choice not has physical motivations, but just for simplicity. Here we would like to point out that the anisotropies D_i^A and D_j^B are different, although they have the same strength, but the difference lies in the values of the parameters p and q, which indicate the percentage of the sites in the sublattices with the presence of such anisotropies.

In our simulations were used square lattice sizes ranging from $L = 20$ up to 128. These lattices consist in two interpenetrating sublattices, each one containing $L^2/2$ sites with periodic boundary conditions. The initial states of the system were prepared in a totally random manner and updated by the Metropolis algorithm [49]. For each sample of the system, the strength of the random single-ion anisotropy D were distributed in the sublattices according to the probability distribution functions given by equations (2) and (3). For example, the case $p = 0.25$ means that 25% of the spins in the sublattice A are free of the influence of random single-ion anisotropy D and another 75% of the spins are under action of the such anisotropy. On the other hand, when $q = 0.75$ we have the case where 75% of the spins in the sublattice B are free of the influence of the single-ion random anisotropy D and the 25% of the remaining spins are under the action of this random anisotropy. Typically, we used 5.0×10^5 MCs (Monte Carlo steps) for the calculation of average values of thermodynamic quantities of interest, after discard 1.0×10^5 MCs for thermalization. Here, 1 MCs means L^2 trials to change the state of a spin of the lattice. After thermalization, the average over the disorder was done using 100 independent samples for any size lattice. Although not shown in the figures, the error bars are smaller than the symbol sizes.

We have calculated the sublattice magnetizations per site, m_A and m_B, defined as

$$m_A = \frac{2[\langle M_A \rangle]}{L^2} = \frac{2\left[\left\langle \sum_A S_i^A \right\rangle\right]}{L^2}, \quad (4)$$

and

$$m_B = \frac{2[\langle M_B \rangle]}{L^2} = \frac{2\left[\left\langle \sum_B S_j^B \right\rangle\right]}{L^2}, \quad (5)$$

where $\langle \cdots \rangle$ denotes thermal averages and $[\cdots]$ denotes average over the samples of the system. The total magnetization per site m_T is defined as

$$m_T = \frac{[\langle M \rangle]}{L^2} = \frac{[\langle M_A + M_B \rangle]}{L^2} = \frac{|m_A + m_B|}{2}. \quad (6)$$

Since, for ferrimagnetic systems, the total magnetization m vanishes in the ordered phase where we have intend to observe the compensation temperature. Therefore, we defined another order parameter that is convenient, the staggered magnetization per site, m_S, which is given by

$$m_S = \frac{[\langle M \rangle]}{L^2} = \frac{[\langle M_A - M_B \rangle]}{L^2} = \frac{|m_A - m_B|}{2}. \quad (7)$$

Further, we also have calculated the following thermodynamics quantities, the specific heat per site

$$c = \frac{[\langle E^2 \rangle] - [\langle E \rangle]^2}{k_B T^2 L^2}, \tag{8}$$

where k_B is the Boltzmann constant and E the total energy of the system. The total and staggered susceptibility are denoted by, χ_T and χ_S, respectively. They are given by:

$$\chi_T = \frac{[\langle M_T^2 \rangle] - [\langle M_T \rangle]^2}{k_B T L^2}, \tag{9}$$

and

$$\chi_S = \frac{[\langle M_S^2 \rangle] - [\langle M_S \rangle]^2}{k_B T L^2}. \tag{10}$$

In order to find the critical point, we used the total U_L^T and staggered U_L^S fourth-order Binder cumulants [50] defined by:

$$U_L^T = 1 - \frac{[\langle M_T^4 \rangle]}{3[\langle M_T^2 \rangle]^2}, \tag{11}$$

and

$$U_L^S = 1 - \frac{[\langle M_S^4 \rangle]}{3[\langle M_S^2 \rangle]^2}. \tag{12}$$

The transition temperature also can be estimated by the position of the peaks of the response functions c and χ_S, but to obtain with greater accuracy in some cases, we have used the intersection of the curves of fourth-order Binder cumulants for different lattice sizes L.

The total magnetization per site m_T vanishes at the compensation temperature T_{comp} [36, 37]. Then, the compensation point can be determined by looking for the crossing point between the absolute values of the sublattice magnetizations. Therefore, at the compensation point, we must have

$$|m_A(T_{comp})| = |m_B(T_{comp})|, \tag{13}$$

and

$$\text{sign}[m_A(T_{comp})] = -\,\text{sign}[m_B(T_{comp})]. \tag{14}$$

We also require that $T_{comp} < T_c$, where T_c is the critical point temperature. These conditions show that at T_{comp} , the A and B sublattice magnetizations cancel each other, whereas at T_c both are zero.

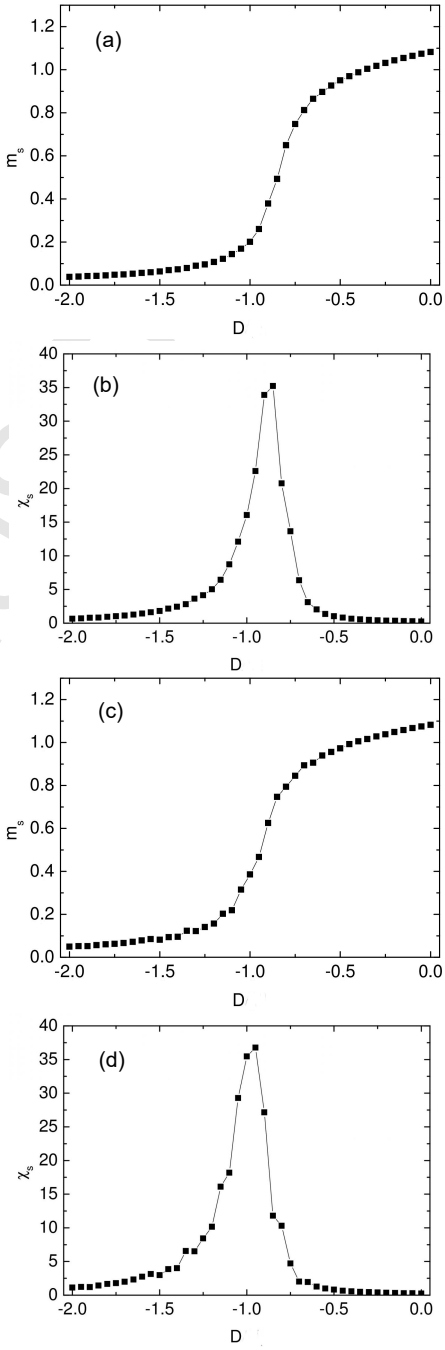

FIG. 1. Staggered magnetization m_S and susceptibility χ_S as a function of strength of the random single-ion anisotropy D and for fixed temperature $T = 2.0$. (a) and (b) are for $p = 0.25$ and $q = 0$. (c) and (d) for $p = 0$ and $q = 0.25$. All data were obtained for a lattice size $L = 40$.

III. RESULTS AND DISCUSSIONS

The behavior of the magnetization play a crucial role in obtaining to finite temperature the phase diagram of the system. The phase diagram, temperature T versus strength of the random single-ion anisotropy D, presents curves in which one part is almost parallel to the D-axis and another that is almost parallel to the T-axis. Thus, for some situations is better to obtain the behavior of the magnetization m as a function of strength of the random single-ion anisotropy D than as a function of temperature T, and vice versa. Therefore, in the region where the curve is parallel to the D-axis, we determined the

critical point by observing the behavior of the magnetization m as a function of temperature T and in the region where the curve is parallel to the T-axis we observe the behavior of the magnetization m as a function of strength of the random single-ion anisotropy D. In this work the temperatures and the strength of the random single-ion anisotropies are measured in units of $|J|/k_B$ and $|J|$, respectively. The p and q are dimensionless parameter.

Firstly, we have shown in Fig. 1 that the staggered magnetization m_S curves go to zero continuously separating the ferrimagnetic from the paramagnetic phase (second-order phase transition) and the strength of the random single-ion anisotropy D at which magnetizations become zero is a critical strength of the random single-ion anisotropy D_c. Thus, the Fig. 1 presents the staggered magnetization m_S (Figs. 1(a) and (c)) and the staggered susceptibility χ_S (Figs. 1(b) and (d)) as a function of strength of the random single-ion anisotropy D and for a fixed temperature $T = 2.0$. In Figs. 1(a) and (b) the data are for $p = 0.25$ and $q = 0$, while in Figs. 1(c) and (d) are for $p = 0$ and $q = 0.25$. Therefore, in order to identify better the second- and first-order transitions lines and compensation temperatures, it should be also studied the thermal behaviors of the magnetizations.

The critical temperatures can be determined by the intersection of the fourth-order Binder cumulants for several lattices sizes or by the position of staggered susceptibility χ_S peaks. To study the phase transition in more detail, we calculate the intersection of the staggered fourth-order Binder cumulants U_L^S to estimate the critical temperature T_c in which the transition occurs. According to the theory of finite size scaling for continuous phase transitions, the behavior of finite size is governed by the ratio L/ξ where ξ is the correlation length. The scaling relation for the fourth-order cumulant shows that, at the critical temperature, where the correlation length is infinite, all curves must intersect at a single point, since the ratio L/ξ is zero for all sizes L [50]. In order to find the critical temperature, we plotted (see Fig. 2) the cumulants U_L^S versus temperature T for several system sizes L, as indicated in the figures. Our estimate for the dimensionless critical temperature with strength of the random single-ion anisotropy fixed $D = -1.0$ is $T_c = 1.884 \pm 0.005$ for $p = 0.25$, $q = 0$ [Fig. 2(a)] and $T_c = 1.938 \pm 0.004$ for $p = 0$, $q = 0.25$ [Fig. 2(b)]. We have chosen these values to take as an example of the phase transitions which occur in the system.

We also obtained the phase diagram of the system, critical temperature T_c as a function strength of the random single-ion anisotropy D, as shown in Fig. 3 and it was determined from the position of the staggered susceptibility χ_S peaks by standard MC simulation for a fixed lattice size $L = 40$. The results were obtained for some selected values of parameters p and q, as indicated in the figure. We also included the limit cases, for $p = q = 1.0$ (pure model) solid line where critical temperature is constant for any values of single-ion anisotropies D and the case $p = q = 0$ [48], black-square point line. In the case of

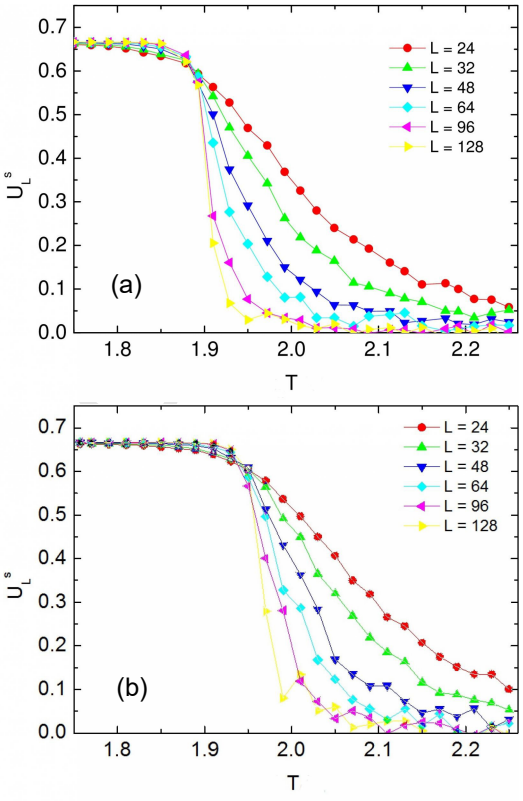

FIG. 2. Staggered fourth-order Binder cumulants U_L^S as a function of temperature T for various lattice sizes L, as indicated in the figures. (a) We have obtained the critical temperature $T_c = 1.884 \pm 0.005$ for $p = 0.25$ and $q = 0$. (b) The critical temperature is $T_c = 1.988 \pm 0.004$ for $p = 0$ and $q = 0.25$. All data were obtained for the strength of the random single-ion anisotropy fixed $D = -1.0$.

$D = 0$, we estimated the critical temperature by crossing fourth-order Binder cumulants for different lattice sizes and found $T_c = 2.36 \pm 0.01$. These results are in good agreement with the one found in the literature [48]. In the case $q = 0$ and $p \neq 0$, the critical temperature line T_c does not vanishes at $D = -2.0$ as in case $p = 0$ and $q = 0$, but tends to a fixed value that depends of p. For example, for the case $q = 0$ and $p = 0.25$ the critical temperature tends to a constant value, $T_c = 0.26 \pm 0.01$, for $D \leq -2.0$. We have observed this same behavior for other cases $p = 0$ and $q \neq 0$. When p and $q \to 1.0$, we found a value for the critical temperature constant $T_c = 2.36 \pm 0.01$ independent of the strength of the random single-ion anisotropy D and which is the same value for the case with $D = 0$. We also observed that for $D \geq 0$ favours the states $\pm 3/2$, i.e., $D \to +\infty$ the sublattice A with spin-3/2 behaves as a two level system with $\pm 3/2$ states. On the other hand, in the region where $D \to -\infty$ the states $\pm 3/2$ are suppressed and the system becomes equivalent to a mixed-spin Ising model with spin-1 and spin-1/2, in cases where the parameter q is large, which leaves most of the spins $S = 1$ out of the influence of the anisotropy D in the sublattice B . We did not find

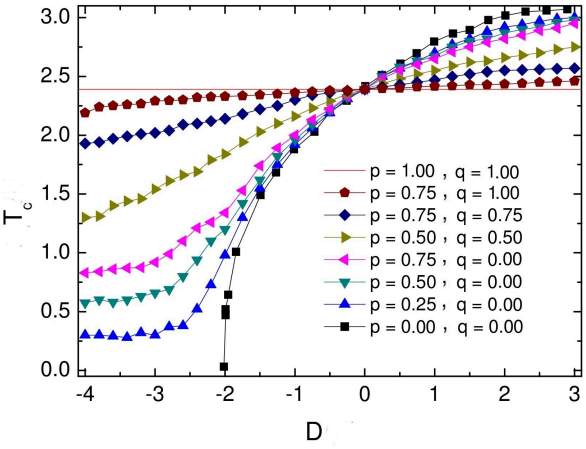

FIG. 3. Phase diagram critical temperature T_c as a function of the strength of the random single-ion anisotropy D for several values of p and q, as indicated in the figure. The solid and black-square point lines represent the limit cases, $p = q = 1.0$ and $p = q = 0$, respectively. The point where all the lines intersect is given by $(D = 0,\ T_c = 2.36 \pm 0.01)$. All lines are second-order phase transitions.

first-order transitions, as we can see in Fig. 1, where staggered magnetization and susceptibility as functions of the strength anisotropy D are always all continuous for any values of p and q. The phase digram of the system exhibits only second-order phase transition lines for any values of p and q.

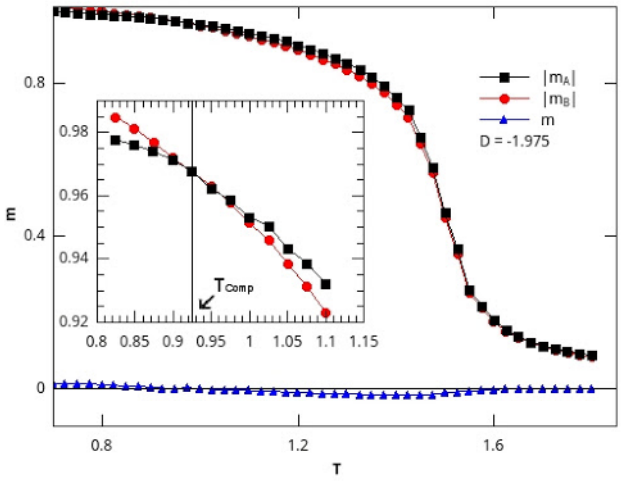

FIG. 4. Total m and sublattice m_A, m_B magnetizations as a function of temperature T for $p = 1.0$, $q = 0$ and $D = -1.975$. In the insets we show the crossing of the sublattice magnetizations. The compensation temperature is shown in the figure and it is $T_{comp} = 0.84 \pm 0.01$.

The compensation temperature is a temperature below the critical point in which the total magnetization vanishes. To see the presence of a compensation point in this system, we shown in Fig. 4 the total m and sublattice m_A, m_B magnetizations as a function of the temperature, for selected values of the parameters $p = 1.0$, $q = 0$ and $D = -1.975$, and we have found $T_{comp} = 0.84 \pm 0.01$ for compensation temperature. T_{comp} exists only for the case $p \neq 0$ and $q = 0$, i. e., the case that all spins of the sublattice B suffer action of the strength of the random single-ion anisotropy D.

We calculated the compensation temperature T_{comp} as a function of strength of the random single-ion anisotropy D and for various values of p and for $q = 0$, as can be seen in Fig. 5. For the case $p = q = 0$, which corresponds to the case with uniform anisotropy, the system presents the multicompensation behavior, as can see in reference [48]. On the other hand, for some $p \neq 0$ and $q = 0$, we found only one compensation temperature T_{comp} in the following range of $-1.98 \leq D \leq -1.90$ for $p = 1.0$ (down diamond points), $-1.98 \leq D \leq -1.93$ for $p = 0.75$ (up diamond points), $-1.98 \leq D \leq -1.97$ for $p = 0.50$ (circle points). Now, for the case $p = 0.25$ (square points), the system exhibits a multicompensation behavior and we obtained two compensation temperatures for some values of D, $-1.97 \leq D \leq -1.962$. Indeed, when p increases (the concentration of the spins on the sublattice A under the influence of random single-ion anisotropy decreases) and the range where the compensation temperature occurs it is also increased.

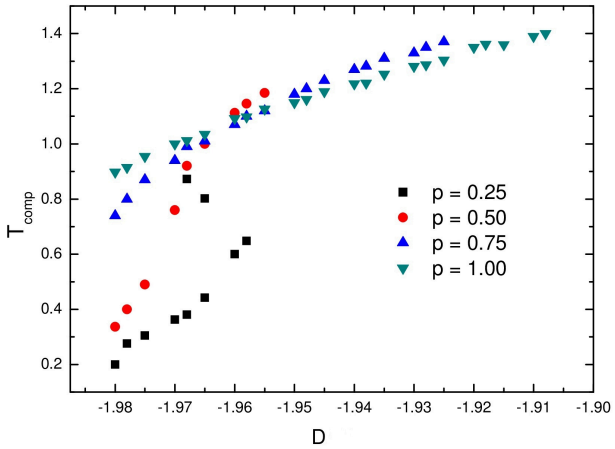

FIG. 5. Compensation temperature T_{comp} as a function of the strength random single-ion anisotropy D for several values of p , as indicated in the figure, and $q = 0$.

IV. CONCLUSIONS

In this work, we have studied the effects of two different random single-ion anisotropies in the mixed spin-1 and spin-3/2 Ising ferrimagnetic system in a square lattice. We have employed the MC simulation. We considered the strength of the random single-ion anisotropy $D = D_A = D_B$ on the sublattices A and B governed by a bimodal probability distribution $P(D_i^A)$ and $P(D_j^B)$, respectively.

The case in which D is an uniform anisotropy, the phase diagram of the system shown only second-order phase transition by MC simulation [48] differently that results from mean-field theory [28] where the phase transitions are first- and second-order. Here, in the our case in which the strength of the single-ion anisotropy D is randomly distributed, we found also a result different from mean-field theories [28, 29] and similar to MC simulation in [48], namely, the phase digram of the system exhibits only second-order phase transition lines for any values of p and q. The compensation temperatures appear only in the case where $q = 0$, namely, in the case all sites of the sublattice B suffers the influence of D, which occurring for a range of $1.98 \leq D \leq 1.90$ and for parameter $0 < p \leq 1.0$. We shown also the system exhibits a multicompensation behavior for $p = 0.25$ and $q = 0$.

V. ACKNOWLEDGMENTS

The authors acknowledge financial support by the Brazilian agencies CNPq, CAPES and FAPEMAT.

[1] M. Blume, Phys. Rev. **141**, 517 (1996).
[2] H. W. Capel, Physica **32**, 966 (1966).
[3] M. Blume, V. J. Emery, and R. B. Griffiths, Phys. Rev. A **4**, 1071(1971).
[4] T. Iwashita and N. Uryu, Phys. Soc. Japan **53**, 721 (1984).
[5] H. F. Verona de Andrade, F. C. Sá Barreto, and J. A. Plascak, Physica A **149**, 606 (1988).
[6] T. Kaneyoshi and Y. Nakamura, J. Phys.: Condens. Matter **10**, 3003 (1998).
[7] T. Kaneyoshi and S. Shin, J. Phys.: Condens. Matter **10**, 7025 (1998).
[8] J. S. Miller, J. C. Calabrese, R. W. Bigelow, A. J. Epstein, J. H. Zhang, S. Chittipeddi, and W. M. Reiff, Chem. Commun. 1026 (1996).
[9] O. Kahn, *Molecular Magnetism*, (VCH, New York, 1993).
[10] J. S. Miller and A. J. Epstein, Angew. Chem. Int. Ed. Engl. **33**, 385 (1994).
[11] Y. T. Chong, D. Gorlitz, S. Martens, M. Y. Eric Yau, S. Allende, J. Bachmann, and K. Nielsch , Adv. Mater. **22**, 2435 (2010).
[12] F. Xu, P. W. Huang, J. H. Huang, R. T. Huang, W. N. Lee, T. S. Chin, and Y. W. Du, Solid State Commun. **151**, 169 (2011).
[13] T. M. Whitney, P. C. Searson, J. S. Jiang, C. L. Chien, Science **261**, 1316 (1993).
[14] H. W. Wu, C. J. Tsai, and L. J. Chen, Appl. Phys. Lett. **90** 043121 (2007).
[15] T. Kaneyoshi, J. Phys. Soc. Japan **56**, 2675 (1987).
[16] T. Kaneyoshi, J. Magn. Magn. Mater. **9**2, 59 (1990).
[17] Y. Nakamura, S. Shin, and T. Kaneyoshi, Physica B **284**, 1479 (2000).
[18] G. Wei, Q. Zhang, Z. Xin, and Y. Liang, J. Magn. Magn. Mater. **277**, 1 (2004).
[19] A. Benyoussef, A. El Kenz, and T. Kaneyoshi, J. Magn. Magn. Mater. **131**, 173 (1994).
[20] A. Benyoussef, A. El Kenz, and T. Kaneyoshi, J. Magn. Magn. Mater. **131**, 179 (1994).
[21] A. Bobák and M. Jurčišin, Physica A **240**, 647 (1997).
[22] A. Bobák, Physica A **258**, 140 (1998).
[23] D. C. de Oliveira, A. A. P. da Silva, D. F. de Albuquerque, and A. S. de Arruda, Physica A **386**, 205 (2007).
[24] T. Kaneyoshi, M. Jascur, and P. Tomczak, J. Phys. Condens. Matter **4**, L653 (1992).
[25] T. Kaneyoshi, Physica A **205**, 677 (1994).
[26] H. K. Mohamad, E. P. Domashevskaya, and A. F. Klinskikh, Physica A **388**, 4713 (2009).
[27] J. S. da Cruz Filho, M. Godoy, and A. S. de Arruda, Physica A **392**, 6247 (2013).
[28] O. F. Abubrig, D. Horvath, and A. Bobák, M . Jascur, Physica A **296**, 437 (2001).
[29] I. J. Souza, P. H. Z. de Arruda, M. Godoy, L. Craco, and A. S. de Arruda, Physica A **444**, 589 (2016).
[30] S. G. A. Quadros and S. R. Salinas, Physica A **206**, 479 (1994).
[31] G. M. Zhang and C. Z. Yang, Phys. Rev. B **48**, 9452 (1993).
[32] G. M. Buendia and M. A. Novotny, J. Phys.: Condens. Matter **9**, 5951 (1997).
[33] G. M. Buendia and J. A. Liendo, J. Phys.: Condens. Matter **9**, 5439 (1997).
[34] Y. Nakamura, J. Phys.: Condens. Matter **12**, 4067 (2000).
[35] Y. Nakamura, Phys. Rev. B **62**, 11742 (2000).
[36] M. Godoy and W. Figueiredo, Phys. Rev. E **65**, 026111 (2002).
[37] M. Godoy, V. S. Leite and W. Figueiredo, Phys. Rev. B **69**, 054428 (2004).
[38] V. S. Leite, M. Godoy and W. Figueiredo, Phys. Rev. B **71**, 094427 (2005).
[39] G. Wei, Q. Zhang, and Y. Gu, J. Magn. Magn. Mater. **301**, 245 (2006).
[40] G. Wei, Y. Gu, and J. Liu, Phys. Rev. B **74**, 024422 (2006).
[41] M. Žukovič and A. Bobák, J. Magn. Magn. Mater. **322**, 2868 (2010).
[42] J. A. Reyes, N. de La Espriella, and G. M. Buendía, Phys. Status Solidi B **10**, 252 (2015).
[43] N. de La Espriella, C. A. Mercado, and J. C. Madera, J. Magn. Magn. Mater. **401**, 22 (2016).
[44] J. Li, A. Du, and G. Z. Wei, Phys. Status Solidi B **238**, 191 (2003).
[45] J. Li, A. Du, and G. Z. Wei, Physica B **348**, 79 (2004).
[46] J. S. da Cruz Filho, T. M. Tunes, M. Godoy, and A. S. de Arruda, Physica A **450**, 180 (2016).
[47] W. P. da Silva, P. H. Z. de Arruda, T. M. Tunes, M. Godoy, and A. S. de Arruda, Physica A **450**, 180 (2016).
[48] M. Žukovič and A. Bobák, Physica A **389**, 5401 (2010).
[49] N. Metropolis, A. Rosenbluth, M. Rosenbluth, A. Teller and E. Teller, J. Chem. Phys. **21**, 1087 (1953).

[50] D. P. Landau and K. Binder, *A Guide to Monte Carlo Simulations in Statistical Physics*, (Cambridge University Press, New York, 2005).